

Decentralized Optimal Demand-Side Management for PHEV Charging in a Smart Grid

Yuting Mou, Hao Xing, *Student Member, IEEE*, Zhiyun Lin, *Senior Member, IEEE*,
and Minyue Fu, *Fellow, IEEE*

Abstract—Plug-in hybrid electric vehicles (PHEV) are expected to become widespread in the near future. However, high penetration of PHEVs can overload the distribution system. In smart grid, the charging of PHEVs can be controlled to reduce the peak load, known as demand-side management (DSM). In this paper, we focus on the DSM for PHEV charging at low-voltage transformers (LVTs). The objective is to flatten the load curve of LVTs, while satisfying each consumer's requirement for their PHEV to be charged to the required level by the specified time. We first formulate this problem as a convex optimization problem and then propose a decentralized water-filling-based algorithm to solve it. A moving horizon approach is utilized to handle the random arrival of PHEVs and the inaccuracy of the forecast nonPHEV load. We focus on decentralized solutions so that computational load can be shared by individual PHEV chargers and the algorithm is scalable. Numerical simulations are given to demonstrate the effectiveness of our algorithm.

Index Terms—Decentralized convex optimization, demand-side management (DSM), plug-in hybrid electric vehicle (PHEV), smart grid, water filling.

I. INTRODUCTION

ROAD TRAFFIC is known as one of the main causes of greenhouse gas emission. Together with the rising fuel price and high-energy efficiency, electric vehicles tend to become more widespread in the next decades. To satisfy the need of long distance travel, plug-in hybrid electric vehicles (PHEVs) are more desirable. A PHEV uses both batteries and a combustion engine to minimize the fuel consumption. A PHEV is charged when it is plugged into the charger located at home or a public charging station. However, this may pose

Manuscript received January 26, 2014; revised April 27, 2014 and August 10, 2014; accepted October 9, 2014. Date of publication October 29, 2014; date of current version February 16, 2015. This work was supported in part by the National Natural Science Foundation of China under Grant 61273113, and in part by the Zhejiang Provincial Natural Science Foundation of China under Grant LR13F030002. Paper no. TSG-00058-2014.

Y. Mou and H. Xing are with the Department of Control Science and Engineering, and the State Key Laboratory of Industrial Control Technology, Zhejiang University, Hangzhou 310027, China (e-mail: ytmou@zju.edu.cn).

Z. Lin is with the College of Electrical Engineering and the State Key Laboratory of Industrial Control Technology, Zhejiang University, Hangzhou 310027, China.

M. Fu is with the School of Electrical Engineering and Computer Science, University of Newcastle, Callaghan, NSW 2308, Australia; and also with the State Key Laboratory of Industrial Control Technology and the Department of Control Science and Engineering, Zhejiang University, Hangzhou 310027, China.

Color versions of one or more of the figures in this paper are available online at <http://ieeexplore.ieee.org>.

Digital Object Identifier 10.1109/TSG.2014.2363096

challenge to the electric grid's distribution system [1]. Large penetration of PHEVs will add to the current peak load or create new peak load. It can cause serious voltage deviation and overloading of transformers. Excessive voltage deviation can cause damage to electrical appliances while persistent overloading can overheat transformers, which may result in a blackout.

Fortunately, with the development of smart grid, advanced metering and communication systems enable us to develop better algorithms to deal with these problems. So the timing and rate of PHEV charging can be controlled to reduce the peak load, which is called demand-side management (DSM). DSM refers to techniques that attempt to influence customer consumption patterns of electricity to match current or forecast capabilities of the power supply system [2]. DSM is surely a critical part of smart grid, as it makes the grid more economical, reliable, and eco-friendly.

There have been a number of studies on DSM of PHEVs. Reference [3] presents a hierarchical control algorithm to realize the synergy between PHEV charging and wind power. The three-level controller proposed in this paper utilizes PHEV charging to compensate wind power fluctuation and thus indirectly regulate the grid frequency. References [4] and [5] deal with the valley-filling problem by controlling the charging of a large population of PHEVs. In [4], a decentralized algorithm is developed based on Nash equilibrium, but only proves optimal in the homogeneous case where all PHEVs have the same exit time, energy need, and maximum charging power. In [5], a control signal from the utility company is altered to guide the updates of PHEVs' charging profiles. This algorithm converges to optimal charging profiles in both homogeneous and nonhomogeneous cases. However, if communication between the utility company and PHEVs is asynchronous, the performance of the algorithm can be largely affected. Moreover, it is complex for engineering practice. References [6] and [7] are more relevant to this paper since they both tackle the problem of distribution transformer overheating. In [6], peak load shedding is utilized to do load shaping, with consideration of consumers' preferences and load priorities. A multiagent system solution is adopted in [7], which features high adaptability and scalability. As both of them address this problem in terms of control strategy, we feel obliged to give a decentralized algorithm to solve this problem quantitatively, which is also simple for engineering practice. Reference [8] gives a comprehensive review on PHEV charging problems.

Finite horizon optimization is a real-time optimization technique which aims to find an optimal control sequence $\{u_k, u_{k+1}, \dots, u_{k+N-1}\}$, which begins at the current time k and ends at some future time $k + N - 1$. To help handle possibly unexpected changes in the system after time k , typically only u_k is applied, whereas $u_{k+1}, \dots, u_{k+N-1}$ are discarded. That is, the aforementioned finite horizon optimization is repeated at each time k to derive the optimal u_k . This is known as moving horizon optimization [9], which is very similar to model predictive control (MPC) [10]. MPC is quite popular in the process control industry. With the development of distributed MPC [11], [12], this method finds applications in many other areas, such as power systems, water distribution systems, and traffic systems [13]–[15]. There have already been some research on distributed optimization within a MPC framework, such as [16].

In this paper, we focus on the impact of PHEV charging on low-voltage transformers (LVTs). The objective is to flatten the load curve of every LVT, while each consumer's requirement for their PHEV to be charged to the required level by the specified time is satisfied. Inspired by the water-filling principle in information theory, we first formulate the PHEV charging problem as a convex optimization problem and then propose a decentralized water-filling-based algorithm to solve it. A moving horizon approach is adopted to handle the random arrival of PHEVs and the inaccuracy of forecast nonPHEV load. In the algorithm, a LVT is only responsible for communication and requiring very little computation while the PHEVs connected to it share the computation in a distributed fashion. Our algorithm will be demonstrated using several numerical simulations, which include academic examples to show the optimality behavior of the proposed algorithm and a practical example to show the effectiveness of our algorithm for DSM.

The rest of this paper is organized as follows. In Section II, the model of PHEV charging is introduced and the problem formulation is presented. In Section III, we give a water-filling algorithm and its modified version to address this problem. Numerical simulations are given in Section IV. The conclusion is given in Section V.

II. PRELIMINARIES AND PROBLEM FORMULATION

In this section, we first give the dynamic model of PHEV charging and then introduce the charging methods of Lithium-ion batteries, moving horizon optimization, and the water-filling principle. Finally, the DSM problem for PHEV charging at LVTs is formulated as an optimization problem.

A. Dynamic Model of PHEV Charging

Nowadays, almost all PHEVs use Lithium-ion batteries because of its advantages, e.g., high-energy density, good load characteristics, and low maintenance.

The state of charge (SOC) is the equivalent of a fuel gauge for the battery in a PHEV and is defined as

$$\text{SOC} = \frac{C_R}{C} \times 100\% \quad (1)$$

with C representing the battery energy capacity (kWh) and C_R is the remaining battery energy capacity (kWh).

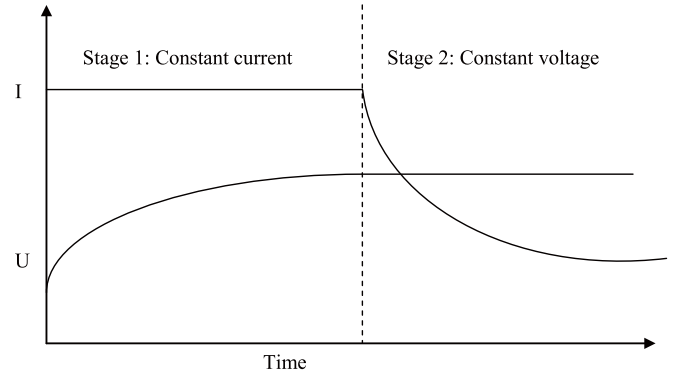


Fig. 1. CC-CV charging process of Lithium-ion batteries (I, current; U, voltage).

Suppose there are n households, each having a PHEV. Suppose, we start at time 0 and the sampling period is set to be ΔT . For the i th PHEV, the initial SOC, target SOC, exit time, battery capacity, charging efficiency coefficient, and maximum charging power are denoted by $x_i(0), x_i^*, T_i = K_i \Delta T, C_i, \eta_{\text{eff}_i} (\in (0, 1))$, and $p_{i,\text{max}} (\geq 0)$, respectively. For households without active PHEVs, their capacities and maximum charging powers will be set to zero. The dynamic model for the i th charging PHEV is given by

$$x_i(k+1) = x_i(k) + \frac{\eta_{\text{eff}_i} \Delta T}{C_i} p_i(k) \quad (2)$$

where $x_i(k)$ and $p_i(k)$ are the SOC and charging power, respectively, at time k . The charging power is assumed to be kept constant in each sampling interval. We assume the efficiency coefficient η_{eff_i} to be constant regardless of the charging power because the efficiency can reach more than 95% if the charging power is not too high [17].

Denoting

$$a_i = \begin{cases} \eta_{\text{eff}_i} \Delta T / C_i & C_i > 0 \\ 0 & C_i = 0 \end{cases}$$

(2) can be rewritten as

$$x_i(k+1) = x_i(k) + a_i p_i(k) \quad (3)$$

which is valid for all PHEVs, whether charging or not. The constraint on $p_i(k)$ is given by

$$0 \leq p_i(k) \leq p_{i,\text{max}}(k) \quad (4)$$

with

$$p_{i,\text{max}}(k) = \begin{cases} p_{i,\text{max}} & k < K_i \text{ and } C_i > 0 \\ 0 & \text{otherwise.} \end{cases}$$

B. Charging Method

Traditionally, constant current constant voltage (CC-CV) charging method is used to charge PHEVs, as shown in Fig. 1. First, the PHEV is charged with a constant current and when the battery voltage limit is reached, Stage 2 begins. In terms of SOC, the best functional range of Lithium-ion batteries is from 20% to 85%. Actually, when Stage 1

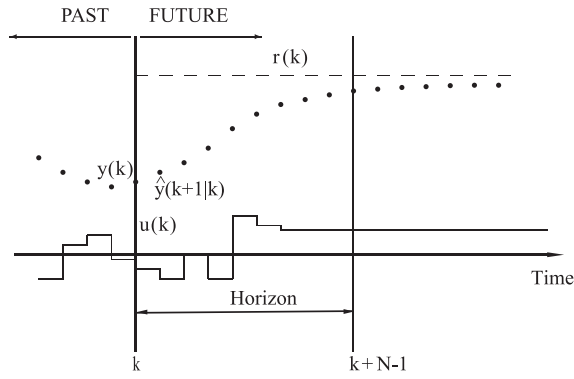


Fig. 2. Moving horizon principle [$r(k)$, reference signal; $y(k)$, output; $\hat{y}(k+1|k)$, predicted output of $k+1$ at k].

terminates, SOC can reach 85%. Thus, it is recommended to ignore Stage 2 [18]. In this paper, PHEVs are charged with variable power. Regarding the effects of variable charging current on Lithium-ion battery, Krieger [17] has given a detailed description in terms of capacity fade and efficiency, from which, we can conclude that Lithium-ion batteries can be charged with dynamic power without adversary effects. Therefore, PHEVs are assumed to be charged by a smart charger, which could determine the charging current of PHEV based on the power allocated and terminal voltage.

C. Moving Horizon

Moving horizon principle means that after computation of the optimal control sequence, only the first control sample will be implemented, subsequently the horizon is shifted one sample and the optimization is restarted with new information of the measurements. Fig. 2 explains the idea of moving horizon. At time k the future control sequence $\{u(k|k), \dots, u(k+N-1|k)\}$ is calculated by optimizing a determined criterion to keep the process as close as possible to the reference signal. This criterion usually takes the form of a quadratic function of the errors between the predicted output signal $\hat{y}(k+1|k)$ and the reference signal $r(k)$. But only the first element of the optimal sequence ($u(k) = u(k|k)$) is applied to the real process. At the next time instant, the horizon is shifted from k to $k+N-1$ to $k+1$ to $k+N$ and a new optimization at time $k+1$ is solved. The process is carried out repeatedly [19].

D. Water Filling

Water filling or water pouring is a well-known algorithm in information theory. As far as we know, this was first put forward in [20]. Many constrained optimization problems can be solved using water filling and it has extended to many other areas, such as case-based reasoning [21], image structural feature extraction [22], and watermarking [23].

The classical water filling algorithm is used to maximize the channel capacity of a communication channel over a finite bandwidth with a given power constraint. Suppose there are M subchannel ($1, 2, \dots, M$) with noise power levels (N_1, N_2, \dots, N_M). The optimization problem is to allocate the

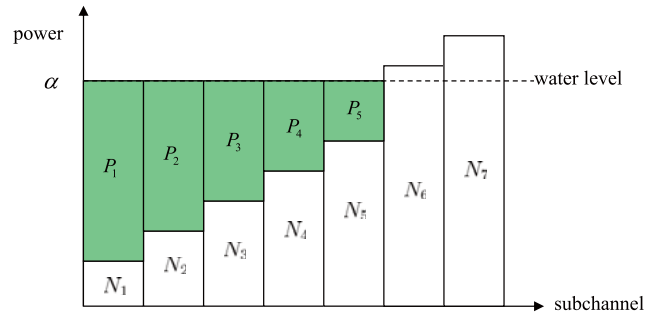


Fig. 3. Water filling for maximizing channel capacity.

power P_i to the i th subchannel for every i , subject to a given total power constraint $\sum_{i=1}^M P_i \leq P_r$. Then the problem can be formulated as [24]

$$\begin{aligned} \max f(P_i) &= \sum_{i=1}^M \log \left(1 + \frac{P_i}{N_i} \right) \\ \text{subject to} & \begin{cases} \sum_{i=1}^M P_i \leq P_r \\ P_i \geq 0, \quad 1 \leq i \leq M. \end{cases} \end{aligned} \quad (5)$$

Using the Lagrange multiplier method to solve this problem, the Lagrangian to be maximized is

$$L(P_i, \lambda) = \sum_{i=1}^M \log \left(1 + \frac{P_i}{N_i} \right) + \lambda \left(P_r - \sum_{i=1}^M P_i \right).$$

Differentiating it with respect to P_i yields

$$\frac{1}{N_i + P_i} - \lambda = 0.$$

Denoting $\alpha = 1/\lambda$ and considering the second constraint $P_i \geq 0, 1 \leq i \leq M$, the solution is given by

$$P_i = \max(0, \alpha - N_i), \quad 1 \leq i \leq M \quad (6)$$

where α is the ‘‘water level’’ chosen to satisfy $\sum_{i=1}^M P_i = P_r$. Equation (6) is the famous water filling result and it can be interpreted by Fig. 3. The important feature of water filling is that P_r is a monotonically increasing function of α , implying that the optimal level of α can be easily found by a simple line search.

E. Problem Formulation

A power distribution system has different kinds of structures, among which the radial structure is the most common one [25]. In this paper, we consider a distribution grid as in Fig. 4, where the distribution grid is hierarchical, involving a high-voltage transformer (HVT) connecting to a set of LVTs, each of which in turn connects to a number of households with PHEV chargers and forms a radial structure, similar to the structure in [7]. The objective is to apply DSM on all PHEV chargers to maximally flatten the power demand curve at the LVT connected to the PHEVs, while satisfying each consumer’s requirement for their PHEV to be charged to the required level by their specified time. As the HVT and LVT may not be able to get the flattest demand curves at the same time and LVTs tend to get overloaded

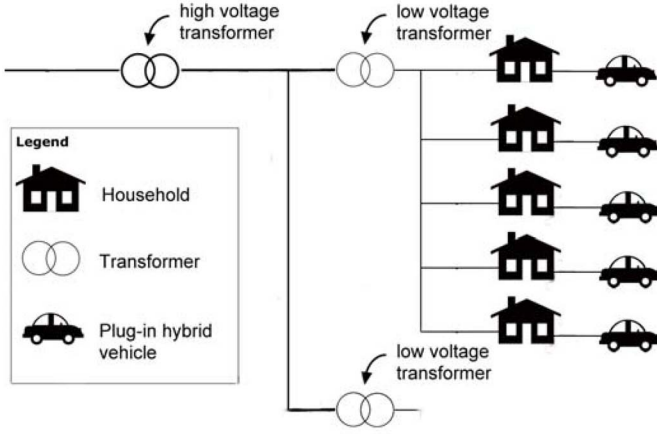


Fig. 4. Schematic of the structure of a distribution grid [7].

sooner than HVTs [7], we consider LVTs only in this paper. We note that there is another structure for power distribution systems, where the grid has multiple LVTs connecting to different household areas. This structure is often used in metropolitan areas because it is of high cost as well as high reliability [25]. We do not consider this structure in this paper.

In this paper, we consider only single-phase LVTs. This is motivated by the facts that power supply to most residential and small commercial customers is single-phase and that all household PHEV chargers are single-phase [25]. (The more powerful three-phase chargers are only equipped at public charging stations, which are not considered here.) It is true that such single-phase power supply may not always come from single-phase LVTs (i.e., it may come from one phase of a two or three-phase LVT). In such a case, load balancing among different phases is managed by a distribution planner, and the main challenge for the distribution planner is to counter the load fluctuations in the individual phases [25], [26]. Therefore, by flattening the demand curve in each phase, load balancing tends to be improved. We also note that coherent DSM for different phases may impose extra difficulties because different phases are often supplied to different residential or commercial areas. Hence, DSM for three-phase power supplies can be effectively treated as three separate DSM problems with single-phase LVTs.

Throughout this paper, we assume that the distribution system has sufficient power capacity so that power line flow limit will not be exceeded. We further assume that the PHEV load is mostly resistive as the power factor of a PHEV charger is very high due to the power factor correction mechanism [27], [28] so that a limit on the voltage drop can be effectively captured by a limit on the power of the load. These assumptions are valid for typical households and LVTs.

We first formulate the PHEV charging problem as a finite horizon optimization problem. Consider the given time horizon from $k = 0$ to $N - 1$, where $N \geq K_i$, $i = 0, 1, \dots, n$. It is assumed that the forecast nonPHEV power consumption $q_i(k)$, $k = 0, 1, \dots, N - 1$, for each household i is known to

the household i . The objective of DSM can be formulated as follows:

$$\begin{aligned} \min f(p) &= \sum_{k=0}^{N-1} \left(\sum_{i=1}^n (p_i(k) + q_i(k)) - \eta \right)^2 \\ \text{subject to } &\begin{cases} \sum_{k=0}^{K_i-1} p_i(k) = b_i \\ 0 \leq p_i(k) \leq p_{i,\max}(k). \end{cases} \end{aligned} \quad (7)$$

The physical meaning of η is the ‘‘ideal’’ flat power curve. The optimization variable is $p_i(k)$, and b_i is the energy need of the i th PHEV by time K_i (normalized by ΔT). Recall (3) and PHEV $_i$ is charged from its initial SOC $x_i(0)$ to its target SOC x_i^* , which is set by the PHEV owner. Then we get

$$x_i^* = x_i(0) + a_i \sum_{k=0}^{K_i-1} p_i(k). \quad (8)$$

So b_i is given by $b_i = (x_i^* - x_i(0))/a_i$. Indeed, $f(p) = 0$ if and only if the aggregate power curve $\sum_{i=1}^n (p_i(k) + q_i(k))$ is flat over k . η is given by

$$\eta = \frac{1}{N} \left(\sum_{i=1}^n b_i + \sum_{k=0}^{N-1} \sum_{i=1}^n q_i(k) \right). \quad (9)$$

Some decentralized or distributed algorithms have been put forward to solve similar problems. Generally, these problems can be divided into two categories: 1) an optimization problem with decoupled cost but a common decision variable and 2) an optimization problem with decoupled cost and sparse coupled constraints [29]. However, the equality constraint of our problem is in a different form, though the objective function can be decoupled.

III. MAIN RESULTS

In this section, we first give a water-filling algorithm for a single PHEV and then develop it into a multiple-PHEV one. A modified version of the second algorithm is also presented. Finally, we consider a more general case where PHEVs can arrive randomly, so the objective function is reformulated and the corresponding algorithm is given.

A. Water Filling for Single PHEV

We drop the subscript because there is only one PHEV. Without loss of generality, we assume the required exit time $K = N$. Using the Lagrange multiplier [30], the Lagrangian of (7) with only one vehicle is given by

$$L(p, \lambda) = \sum_{k=0}^{N-1} (p(k) + q(k) - \eta)^2 + 2\lambda \left(\sum_{k=0}^{N-1} p(k) - b \right) \quad (10)$$

where $b = (x^* - x(0))/a$. The factor of 2 above is for convenience. Differentiating the Lagrangian with respect to $p(k)$ and setting the result to zero yield

$$p(k) + q(k) - \eta + \lambda = 0. \quad (11)$$

Denoting $\alpha = \eta - \lambda$ (which is independent of k), (11) can be rewritten as

$$p(k) + q(k) = \alpha. \quad (12)$$

Algorithm 1 Water Filling for a Single PHEV

Input: ϵ , p_{\max} , b and $q(k)$, $k = 0, 1, \dots, N - 1$
Output: α and $p(k)$, $k = 0, 1, \dots, N - 1$

- 1: Initialize $\alpha_{\min} = \min_k q(k)$ and $\alpha_{\max} = \max_k q(k) + p_{\max}$
- 2: **while** $\alpha_{\max} - \alpha_{\min} > \epsilon$ **do**
- 3: Choose $\alpha = (\alpha_{\min} + \alpha_{\max})/2$
- 4: Compute $p(k) = \mathcal{P}[\alpha - q(k)]$, $k = 0, 1, \dots, N - 1$
- 5: **if** $\sum_{k=0}^{N-1} p(k) > b$ **then**
- 6: set $\alpha_{\max} = \alpha$
- 7: **else if** $\sum_{k=0}^{N-1} p(k) < b$ **then**
- 8: set $\alpha_{\min} = \alpha$
- 9: **end if**
- 10: **end while**

The above is the optimality condition without considering the constraints $0 \leq p(k) \leq p_{\max}$. When these constraints are considered, the optimality condition becomes the following one.

There exists a constant α (which will be called the equi-power level) such that for any $0 \leq k < N - 1$, either (12) holds or

$$p(k) = 0 \text{ and } p(k) + q(k) \geq \alpha \quad (13)$$

or

$$p(k) = p_{\max} \text{ and } p(k) + q(k) \leq \alpha. \quad (14)$$

Remark 1: The optimal solution above can be simply interpreted as the following water filling principle: initialize $\alpha = \min_k q_k$. Then, gradually raise α . Each time α is raised a bit, compute the $p(k) = \alpha - q(k)$ and project it to the feasible region $[0, p_{\max}(k)]$, then compute $\sum_k p(k)$. Gradually, raise α until the sum equals b .

We examine some properties of the water-filling principle. Denote the set $\{0, 1, \dots, N - 1\}$ by \mathcal{N} and decompose it into three disjoint subsets: $\mathcal{N}_1 = \{k \in \mathcal{N} : p(k) = p_{\max}\}$, $\mathcal{N}_2 = \{k \in \mathcal{N} : 0 < p(k) < p_{\max}\}$; $\mathcal{N}_3 = \{k \in \mathcal{N} : p(k) = 0\}$. The three subsets \mathcal{N}_1 , \mathcal{N}_2 , and \mathcal{N}_3 correspond to (14), (12) and (13), respectively. Then Lemma 1 gives properties of the water-filling solution $p(k)$.

Lemma 1: Three properties of the water-filling solution $p(k)$ are given as follows.

- 1) For any $k_1 \in \mathcal{N}_1$, $k_2 \in \mathcal{N}_2$, $k_3 \in \mathcal{N}_3$ (if the subsets are not empty), $q(k_1) < q(k_2) < q(k_3)$ and $q(k_1) + p(k_1) \leq q(k_2) + p(k_2) \leq q(k_3) + p(k_3)$.
- 2) $p(k) + q(k)$ are at equal level for all $k \in \mathcal{N}_2$, if this subset has multiple elements.
- 3) If $q(k) = q(\tilde{k})$ for some $k \neq \tilde{k}$, then $q(k) + p(k) = q(\tilde{k}) + p(\tilde{k})$.

Proof: From (12)–(14), we can infer that $q(k_1) + p(k_1) \leq \alpha$, $q(k_2) + p(k_2) = \alpha$, $q(k_3) + p(k_3) \geq \alpha$, so $q(k_1) + p(k_1) \leq q(k_2) + p(k_2) \leq q(k_3) + p(k_3)$. Note that $p(k_1) = p_{\max}$, $0 < p(k_2) < p_{\max}$, $p(k_3) = 0$, which means $p(k_1) > p(k_2) > p(k_3)$ and considering $q(k_1) + p(k_1) \leq q(k_2) + p(k_2) \leq q(k_3) + p(k_3)$, we infer $q(k_1) < q(k_2) < q(k_3)$. Thus, Property 1 is justified. With regard to Property 2, from (12) we know $p(k) + q(k) = \alpha$ and the equal level is α .

Algorithm 2 Water Filling for Multiple PHEVs

Input: ϵ , $p_{i,\max}$, b_i and $q_i(k)$, $k = 0, 1, \dots, N - 1$, $i = 1, 2, \dots, n$
Output: $p_i(k)$, $k = 0, 1, \dots, N - 1$, $i = 1, 2, \dots, n$

- 1: Every PHEV reports nonPHEV power demand $q_i(k)$ to LVT, $k = 0, 1, \dots, N - 1$, $i = 1, 2, \dots, n$
- 2: LVT computes the aggregate demand $q(k) = \sum_{i=1}^n q_i(k)$, $k = 0, 1, \dots, N - 1$
- 3: **for** $i = 1, 2, \dots, n$ **do**
- 4: PHEV _{i} gets $q(k)$ from LVT, $k = 0, 1, \dots, N - 1$
- 5: PHEV _{i} computes $p_i(k)$ using Algorithm 1, $k = 0, 1, \dots, N - 1$
- 6: PHEV _{i} reports $p_i(k)$ to LVT, $k = 0, 1, \dots, N - 1$
- 7: LVT computes $q(k) \leftarrow q(k) + p_i(k)$, $k = 0, 1, \dots, N - 1$
- 8: **end for**

Finally, as $q(k) = q(\tilde{k})$, k and \tilde{k} must both belong to the same subset. If $k, \tilde{k} \in \mathcal{N}_1$, then $p(k) = p(\tilde{k}) = p_{\max}$. So $q(k) + p(k) = q(\tilde{k}) + p(\tilde{k})$. Similarly, the same conclusion can be drawn if $k, \tilde{k} \in \mathcal{N}_3$. If $k, \tilde{k} \in \mathcal{N}_2$, from Property 2, we also draw the same conclusion. In the conclusion, Property 3 holds. ■

It is easy to see that the optimal value of α can be found using a bi-section method. In Algorithm 1, ϵ has a very small positive value and $\mathcal{P}[\cdot]$ is the projection operation, that is

$$\mathcal{P}[x(k)] = \begin{cases} p_{\max}(k) & x(k) > p_{\max}(k) \\ x(k) & 0 \leq x(k) \leq p_{\max}(k) \\ 0 & x < 0. \end{cases}$$

Note that the number of iterations \mathcal{T} can be calculated as $\epsilon \geq 2^{-\mathcal{T}}(\alpha_{\max} - \alpha_{\min})$, which gives

$$\mathcal{T} \geq \log_2 \left(\frac{\alpha_{\max} - \alpha_{\min}}{\epsilon} \right). \quad (15)$$

For example, if $\alpha_{\max} - \alpha_{\min} = 10$ and set the value of ϵ to 0.01, then $\mathcal{T} \geq \log_2 1000 \approx 10$, i.e., the algorithm will converge in ten iterations.

B. Water Filling for Multiple PHEVs

For the case of multiple PHEVs, the optimal solution is not unique. This is because two PHEVs can “trade” their charging times without affecting the total power consumption. In the following, we give an optimal solution. Without loss of generality, we assume that $K_1 \leq K_2 \leq \dots \leq K_n \leq N$. The main idea is that we do water filling to all the PHEVs one-by-one from 1 to n until all PHEVs are done. Then Algorithm 2 is given.

Remark 2: In Algorithm 2, we only need global information in the initialization steps (Steps 1 and 2) and if $q_i(k)$ is from historical data, we can acquire $q(k)$ directly from the LVT side.

Remark 3: Algorithm 2 is linear in $n\mathcal{T}$, where \mathcal{T} in (15) is the number of iterations for Algorithm 1. Also note that ϵ needs to be chosen sufficiently small for Algorithm 2 to be valid.

Theorem 1: The solution given by Algorithm 2 is optimal when $\epsilon = 0$.

To prove Theorem 1, Lemma 2 is given.

Lemma 2: Consider the case $K_1 = K_2 \dots = K_n = N$ and assume $\epsilon = 0$. Then, the solution of p_i^* , $i = 1, 2, \dots, n$, given by Algorithm 2 is optimal.

Proof: Without loss of generality, we assume that $q(k) = \sum_{i=1}^n q_i(k)$ ($k = 0, 1, \dots, N-1$) is monotonically nondecreasing, i.e., $q(0) \leq q(1) \leq \dots \leq q(N-1)$. If this were not the case, we could sort $q(k)$ and relabel the time indices to make $q(k)$ monotonically nondecreasing. It is clear that the constraints for $p_i(k)$ remain the same after the sorting and relabeling.

We first prove the result for the case of $n = 2$. Denote $p_i = [p_i(0) p_i(1) \dots p_i(N-1)]^T$ and $p = [p_1 p_2]$. We proceed by contradiction. Let $p^* = [p_1^* p_2^*]$ be the solution given by Algorithm 2. That is, p_1^* is optimal for the given q and p_2^* is optimal for $q + p_1^*$. Define

$$\begin{aligned} \mathcal{N}_1 &= \{k \in \mathcal{N} : p_1^*(k) = p_{1,\max}\} \\ \mathcal{N}_2 &= \{k \in \mathcal{N} : 0 < p_1^*(k) < p_{1,\max}\} \\ \mathcal{N}_3 &= \{k \in \mathcal{N} : p_1^*(k) = 0\} \end{aligned}$$

and denote by α^1 the corresponding equip-power level. It is clear that $k_1 < k_2 < k_3$ for all $k_1 \in \mathcal{N}_1, k_2 \in \mathcal{N}_2, k_3 \in \mathcal{N}_3$ (if the subsets are nonempty).

We proceed by contradiction. Suppose p^* is not an optimal solution for the given q . Since p_2^* is optimized using the water filling principle for the given $q + p_1^*$, p^* not being optimal means that we can perturb p_1^* slightly without violating its constraints to further reduce $f(p)$, i.e., p_1^* does not satisfy the water-filling conditions for the given $q + p_2^*$. We show below that this is not possible.

Using Lemma 1, we know that $q(k) + p_1^*(k)$ and $q(k) + p_1^*(k) + p_2^*(k)$ are also monotonically nondecreasing. Consider three cases.

Case 1: \mathcal{N}_2 is empty and \mathcal{N}_1 is nonempty. Denote by $\bar{k}_1 = \max\{k_1 : k_1 \in \mathcal{N}_1\}$. Then, $p_1^*(k) = p_{1,\max}$ for all $k \leq \bar{k}_1$ and $p_1^*(k) = 0$ for all $k > \bar{k}_1$. At the same time, $q(k_1) + p_1^*(k_1) + p_2^*(k_1) \leq q(k_3) + p_1^*(k_3) + p_2^*(k_3)$ for any $k_1 \leq \bar{k}_1 < k_3$, due to the monotonicity. Hence, p_1^* satisfies the water-filling conditions and thus the optimal solution for the given $q + p_2^*$.

Case 2: \mathcal{N}_2 is empty and \mathcal{N}_3 is nonempty. Denote by $\underline{k}_3 = \min\{k_3 : k_3 \in \mathcal{N}_3\}$. Then, $p_1^*(k) = p_{1,\max}$ for all $k < \underline{k}_3$ and $p_1^*(k) = 0$ for all $k \geq \underline{k}_3$. Similar to Case 1, $q(k_1) + p_1^*(k_1) + p_2^*(k_1) \leq q(k_3) + p_1^*(k_3) + p_2^*(k_3)$ for any $k_1 < \underline{k}_3 \leq k_3$, due to the monotonicity. Again, p_1^* is the optimal solution for the given $q + p_2^*$.

Case 3: \mathcal{N}_2 is nonempty. By (12), $q(k_2) + p_1^*(k_2)$ takes the same value α_1 for all $k_2 \in \mathcal{N}_2$. Then by Lemma 1, $p_2^*(k_2)$ takes the same value for all $k_2 \in \mathcal{N}_2$ as well. Denote $\bar{\alpha}_1 = q(k_2) + p_1^*(k_2) + p_2^*(k_2)$ for any (or all) $k_2 \in \mathcal{N}_2$. Then, we have

$$\begin{aligned} p_1^*(k_1) &= p_{1,\max}, \quad q(k_1) + p_1^*(k_1) + p_2^*(k_1) \leq \bar{\alpha}_1, \quad \forall k_1 \in \mathcal{N}_1 \\ 0 &< p_1^*(k_2) < p_{1,\max}, \quad q(k_2) + p_1^*(k_2) + p_2^*(k_2) \\ &= \bar{\alpha}_1, \quad \forall k_2 \in \mathcal{N}_2, \quad p_1^*(k_3) = 0, \quad q(k_3) + p_1^*(k_3) + p_2^*(k_3) \\ &> \bar{\alpha}_1, \quad \forall k_3 \in \mathcal{N}_3. \end{aligned}$$

That is, p_1^* satisfies the water-filling conditions and thus is the optimal solution for the given $q + p_2^*$.

From the above three cases, it is clear that p_1^* is the optimal solution for the given $q + p_2^*$. Combining with the fact that p_2^* is the optimal solution for the given $q + p_1^*$, p^* is a local optimal solution for the given q . Note that the constrained optimization problem for $f(p)$ is convex, thus any local optimal solution is a global optimal solution. Hence, p^* is a global optimal solution for the given q .

Now, we generalize the proof for the case of $n > 2$. Again, we proceed by contradiction. Let $p^* = [p_1^* p_2^* \dots p_n^*]$ be the solution given by Algorithm 2 and suppose it is not optimal. Then, we can perturb some p_i^* , $i < n$ while fixing all other $p_j^*, j \neq i$ such that $f(p)$ can be reduced. We show that this is not possible.

Define $\tilde{q} = q + p_1^* + \dots + p_{i-1}^*$, $\tilde{p}_1 = p_i$, $\tilde{p}_2 = p_{i+1}^* + \dots + p_n^*$. Again, using Lemma 1 repeatedly, we know that $\tilde{q}(k)$, $\tilde{q}(k) + \tilde{p}_1^*(k)$ and $\tilde{q}(k) + \tilde{p}_1^*(k) + \tilde{p}_2^*(k)$ are all monotonically nondecreasing. Define the sets $\mathcal{N}_1^i, \mathcal{N}_2^i$, and \mathcal{N}_3^i similarly as before (but for \tilde{p}_1^*). Then, $\tilde{p}_2(k_2)$ takes the same value for all $k_2 \in \mathcal{N}_2^i$, following from the repeated use of Property 3 of Lemma 1. Then, similar to the three cases above, we can prove that \tilde{p}_1 is optimal for the given $\tilde{q} + \tilde{p}_2^*$. Thus, $f(p)$ can not be reduced by perturbing p_i only. Because i is any value between 1 and n , the above implies that p^* is a local optimal for the given q . By the convexity of the constrained optimization problem for $f(p)$, p^* is a global optimal solution for the given q . ■

Now, we give the proof of Theorem 1 using Lemma 2.

Proof: Set $\epsilon = 0$ and consider the general case of $n \geq 2$. Recall that $K_1 \leq K_2 \leq \dots \leq K_n \leq N$. Let $p^0 = [p_1^0 p_2^0 \dots p_n^0]$ be an optimal solution to (7) for the given q (obtained by any method) and denote by f^0 the minimum value of $f(p)$. Note that the optimizer p^0 for f^0 may not be unique. We show that another optimizer p^* can be obtained by Algorithm 2. To this end, we denote $\tilde{b}_1 = b_1$ and define

$$\tilde{b}_i = \sum_{k=0}^{K_1-1} p_i^0(k), \quad i = 2, \dots, n.$$

Now consider a new problem

$$\begin{aligned} \min f(p) &= \sum_{k=0}^{K_1-1} \left(\sum_{i=1}^n (p_i(k) + q_i(k)) - \eta \right)^2 \\ \text{subject to } &\begin{cases} \sum_{k=0}^{K_1-1} p_i(k) = \tilde{b}_i \\ 0 \leq p_i(k) \leq p_{i,\max}(k). \end{cases} \end{aligned}$$

It is clear from Lemma 2 that an optimal solution for this problem is given by Algorithm 2. Denote the optimal p_1 by p_1^* . It is clear that p_1^* is obtained without knowing $\tilde{b}_2, \dots, \tilde{b}_n$. Once p_1^* is obtained, we add it to q and proceed to optimize p_2 . Following the same argument above, p_2 can be optimized using Algorithm 2 as well without considering the constrains for p_3, \dots, p_n . Repeating the above, it is clear that the solution $p^* = [p_1^* p_2^* \dots p_n^*]$ obtained by Algorithm 2 is an optimal solution for the given q . ■

Remark 4: It is inferred from Theorem 1 (or Lemma 2) that if $K_1 = K_2 \dots = K_n = N$, the result given by Algorithm 2 is optimal no matter in which order they do water filling. If two PHEVs switch the orders in which they do water filling, they trade their charging times. By doing so, a different optimal

Algorithm 3 Modified Water Filling for Multiple PHEVs

Input: P_r , ϵ , $p_{i,\max}$, b_i , $q_i(k)$, $k = 0, 1, \dots, N-1$ and K_i , $i = 1, 2, \dots, n$, $K_0 = 0$

Output: $\bar{p}_i(k)$, $k = 0, 1, \dots, N-1$

- 1: Do water filling as in Algorithm 2 in the first circular order
- 2: LVT computes total power demand at time k : $P_{\text{total}}(k) = \sum_{i=1}^n (q_i(k) + p_i(k))$, $k = 0, 1, \dots, N-1$
- 3: **if** $\exists P_{\text{total}}(k) > P_r$ for some k **then**
- 4: LVT computes $E_{\text{exceed}} = \sum_{k=0}^{N-1} (P_{\text{total}}(k) - P_r)$
- 5: Each PHEV computes $b_i \leftarrow b_i(1 - E_{\text{exceed}} / \sum_{i=1}^n b_i)$
- 6: Go to Line 1.
- 7: **end if**
- 8: Every PHEV i gets its intermediate energy need at time K_1, K_2, \dots, K_{i-1}
- 9: **for** $i = 1, 2, \dots, n$ **do**
- 10: Do water filling as in Algorithm 2 all circular orders during the interval from K_{i-1} to K_i
- 11: Compute $\bar{p}_i(k)$, $k = K_{i-1}, \dots, K_i$
- 12: **end for**
- 13: Get $\bar{p}_i(k)$, $k = 0, 1, \dots, N-1$

solution may be derived. Algorithm 3 in the next section will study how to take advantage of this feature to give a balanced power dispatch among all PHEVs.

C. Modified Water Filling for Multiple PHEVs

Algorithm 2 has two problems, so we will do some modifications in this section. Firstly, the solution given by Algorithm 2 tends to meet the demand of PHEV $_i$ earlier than that of PHEV $_j$ for any $i < j$. This can create a problem if the future supply and demand forecasts become inaccurate or the exit times get altered. It would be more desirable to have a somewhat balanced dispatch of power to all PHEVs. Secondly, although Algorithm 2 maximally flattens the total demand curve, the resulting curve may exceed the capacity limit of the transformer. In the event that the overloading is caused by the excessive demand of the PHEVs, we can avoid overloading by reducing the energy need of every PHEV at the expense of not totally satisfying the customers' needs. These two problems can be addressed by the following modified version of Algorithm 2.

To help describe the modified algorithm, we give the definition of circular order.

Definition 1: Given n numbers, $X_1 \leq X_2 \leq \dots \leq X_n$, then their circular orders includes n different orders and the i th one is $X_i, X_{i+1}, \dots, X_n, X_1, \dots, X_{i-1}$.

Here, we still assume that $K_1 \leq K_2 \leq \dots \leq K_n \leq N$. To deal with the first problem, the idea is to do power allocation in circular orders and allocate power according to the average. More specifically, firstly, do water filling as in Algorithm 2 in the first circular order and get the intermediate energy need at K_1, K_2, \dots, K_{n-1} ; then do water filling in other orders in the interval from 0 to K_1 , K_1 to K_2 , \dots , K_{n-1} to K_n . See Algorithm 3 for details. In the algorithm, the intermediate target need of PHEV $_i$ at K_j is defined to be $b_i(K_j) = \sum_0^{K_j-1} p_i(k)$, where $p_i(k)$ is the power allocated to PHEV $_i$ using Algorithm 2 with the first circular order.

To tackle the second problem, we denote P_r as the rated power of the transformer, or its capacity limit. First, we check whether the total power demand exceeds the capacity limit, and if this is true, we calculate how much energy (E_{exceed}) is charged into the PHEVs during the overloading period. We then compute its ratio to the total energy need of all PHEVs (i.e., $E_{\text{exceed}} / \sum_{i=1}^n b_i$). The energy need of every PHEV will be reduced according to this ratio. This works as a protection mechanism.

Theorem 2: The solution given by Algorithm 3 is optimal when $\epsilon = 0$ and there is no overloading.

To prove Theorem 2, we first give the following lemma.

Lemma 3: Consider the case $K_1 = K_2 = \dots = K_n = N$, do water filling according to Algorithm 2 n times in circular order. The average of the n optimal results is still optimal.

Proof: Optimal solution to the i th PHEV in the j th circular order is denoted by $p_{i,j}^* = [p_{i,j}^*(0) p_{i,j}^*(1) \dots p_{i,j}^*(K_i - 1)]'$ and the average $1/n \sum_{j=1}^n p_{i,j}^*$ is denoted by $\bar{p}_i^* = [\bar{p}_i^*(0) \bar{p}_i^*(1) \dots \bar{p}_i^*(K_i)]'$. First, we prove \bar{p}_i^* still satisfy the two constraints

$$p_{i,j}^*(k) \leq p_{i,\max}(k) \Rightarrow$$

$$\bar{p}_i^*(k) = \frac{1}{n} \sum_{j=1}^n p_{i,j}^*(k) \leq \frac{1}{n} \sum_{j=1}^n p_{i,\max}(k) = p_{i,\max}(k).$$

Similarly, $\bar{p}_i(k) \geq 0$. So $0 \leq p_i(k) \leq p_{i,\max}(k)$ is satisfied

$$\sum_{k=0}^{N-1} p_{i,j}^*(k) = b_i \Rightarrow$$

$$\sum_{k=0}^{N-1} \bar{p}_i^*(k) = \sum_{k=0}^{N-1} \frac{1}{n} \sum_{j=1}^n p_{i,j}^*(k) = \frac{1}{n} \sum_{j=1}^n \sum_{k=0}^{N-1} p_{i,j}^*(k) = b_i.$$

Thus, the equality constraint is also satisfied. We proceed with the proof of optimality. Recall the objective function in (7), $p_{i,j}^*(k)$ being optimal means

$$\sum_{i=1}^n (p_{i,j}^*(k) + q_i(k)) - \eta = M^*(k), \quad j = 1, 2, \dots, n.$$

So

$$\begin{aligned} & \sum_{i=1}^n (\bar{p}_i^*(k) + q_i(k)) - \eta \\ &= \sum_{i=1}^n \left(\frac{1}{n} \sum_{j=1}^n p_{i,j}^*(k) + q_i(k) \right) - \eta \\ &= \sum_{i=1}^n \frac{1}{n} \sum_{j=1}^n p_{i,j}^*(k) + \frac{1}{n} \sum_{j=1}^n \sum_{i=1}^n q_i(k) - \frac{1}{n} \sum_{j=1}^n \eta \\ &= \frac{1}{n} \sum_{j=1}^n \left(\sum_{i=1}^n p_{i,j}^*(k) + \sum_{i=1}^n q_i(k) - \eta \right) \\ &= \frac{1}{n} \sum_{j=1}^n \left[\sum_{i=1}^n (p_{i,j}^*(k) + q_i(k)) - \eta \right] \\ &= \frac{1}{n} \sum_{j=1}^n M^*(k) = M^*(k). \end{aligned}$$

As a result, \bar{p}_i^* is also optimal. ■

Algorithm 4 Water Filling With Moving Horizon

Input: $p_{i,\max}$, b_i and K_i , $i = 1, 2, \dots, n$
Output: $\bar{p}_i(k)$, $i = 1, 2, \dots, n$

- 1: **while** 1 **do**
- 2: Compute $K(k) = \max(K_i)$, $i = 1, 2, \dots, n$
- 3: Do water filling as in Algorithm 3
- 4: Get $\bar{p}_i(k)$, $i = 1, 2, \dots, n$
- 5: $k \leftarrow k + 1$
- 6: **end while**

Then, we give the proof of Theorem 2 using Lemma 3.

Proof: We consider the general case where $K_1 \leq K_2 \leq \dots \leq K_n \leq N$. After doing water filling as in Algorithm 2 in the first circular order every PHEV i gets its intermediate energy needs at times K_1, K_2, \dots, K_{i-1} . Then, for every time interval K_i to K_{i+1} , following the same argument as in the proof of Lemma 2, \bar{p}_i is optimal. ■

D. Water Filling With Moving Horizon

The algorithms above assume that all PHEVs start charging at the same time, but it is unrealistic. In this subsection, we consider the general case where PHEVs can arrive randomly and develop an optimal algorithm based on water filling and moving horizon. First, the objective function in (7) needs some adjustment

$$\begin{aligned} \min f(p) &= \sum_{k=t}^{K(k)-1} \left(\sum_{i=1}^n (p_i(k) + q_i(k)) - \eta(k) \right)^2 \\ \text{subject to } &\begin{cases} \sum_{k=0}^{K_i-1} p_i(k) = b_i \\ 0 \leq p_i(k) \leq p_{i,\max}(k) \end{cases} \end{aligned} \quad (16)$$

where $K(k) \triangleq \max(K_i)$, $i = 1, \dots, n$ at time k and t means the optimization starts from the present time. If PHEV i is not active, K_i will be set to zero. Thus, $K(k)$ will not change until a new PHEV with a relatively late exit time arrives. And $\eta(k)$ is given by

$$\eta(k) = \frac{\sum_{i=1}^n (b_i - b_i(t-1)) + \sum_{k=t}^{K(k)-1} \sum_{i=1}^n q_i(k)}{K(k) - t}. \quad (17)$$

Algorithm 4 is given to address this online optimization problem. Our algorithm is optimal in the sense that for a given k , the objective function in (16) is minimized. Note that this objective function evolves in time.

Remark 5: In Algorithm 4, $\bar{p}_i(k)$ is updated every sample time, but in practice, we can update $\bar{p}_i(k)$ when another PHEV arrives or the forecast of nonPHEV loads change to save calculation and communication.

IV. NUMERICAL SIMULATIONS

In this section, we first give a numerical simulation to illustrate Algorithms 2 and 3. Then, we give an example to illustrate Algorithm 4. The purpose of the examples above is to show how the proposed algorithms work. Finally, realistic power-consumption data are used to demonstrate the effectiveness of our algorithm in flattening LVT load curve.

TABLE I
PARAMETERS OF THE FIVE HOUSEHOLDS

NO.	Max Power	Energy Need	Exit Time	non-PHEV
1	4	20	84	$0.2q$
2	3.5	15	112	$0.3q$
3	3.9	20	112	$0.1q$
4	4.6	25	112	$0.25q$
5	4	20	112	$0.15q$

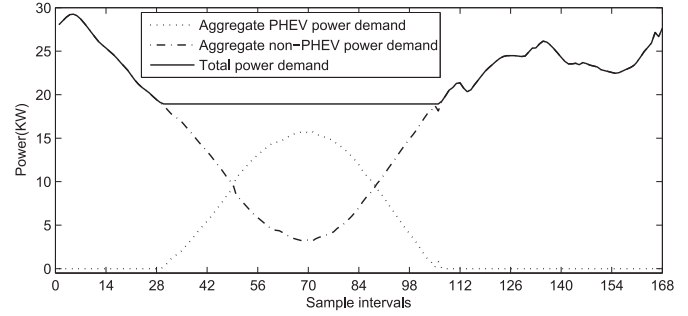


Fig. 5. Power curve from Algorithms 2 and 3.

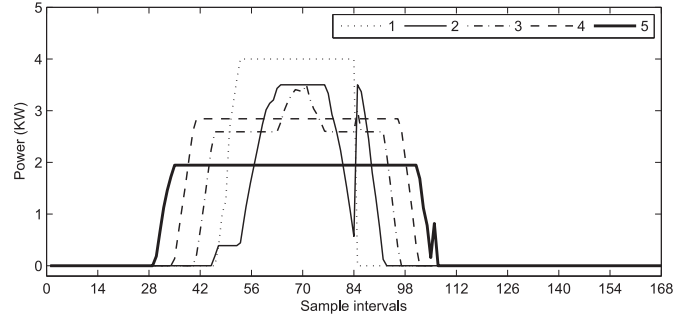


Fig. 6. Power allocation by Algorithm 2.

A. Illustration of Algorithms 2 and 3

We consider five households here and the simulation parameters are given in Table I. The aggregate nonPHEV power demand q is given by the dash-dot curve in Fig. 5, which is from [7]. In the example, the starting time is assumed to be 1, which corresponds to 17:00 h, and the sampling period corresponds to 7 samples/h (i.e., there are 168 samples for 24 h). The unit for power is KW and unit for energy is KWh.

Both Algorithms 2 and 3 can minimize the objective function and flatten the aggregate power curve (see Fig. 5). However, the power allocated to each PHEV is very different for each algorithm. As we have mentioned before, the solution given by Algorithm 2 tends to meet the demand of PHEV i earlier than that of PHEV j for any $i < j$. We can see from Figs. 6 and 7 that Algorithm 3 gives more balanced charging curves than given by Algorithm 2.

B. Illustration of Algorithm 4

In this simulation, random arrival of PHEVs is considered to demonstrate the moving horizon method. The entry and exit times for the PHEVs are shown in Table II. Other parameters are the same as those in the previous subsection.

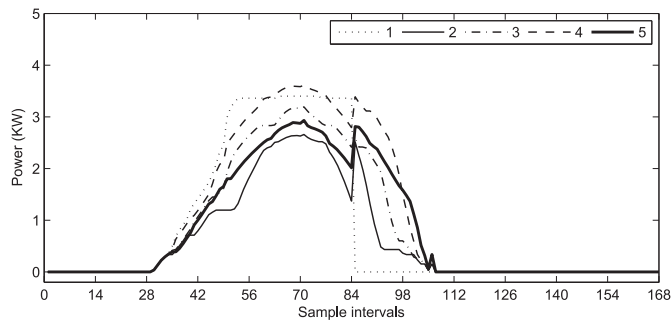


Fig. 7. Power allocation by Algorithm 3.

TABLE II
ENTRY AND EXIT TIMES OF FIVE PHEVS

NO.	1	2	3	4	5
Entry Time	1	1	8	43	50
Exit Time	84	98	105	98	126

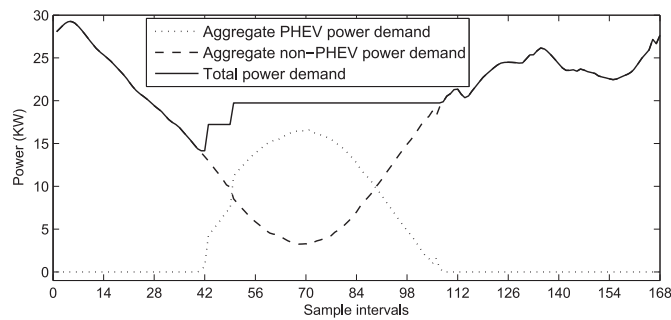


Fig. 8. Power curve from Algorithm 4.

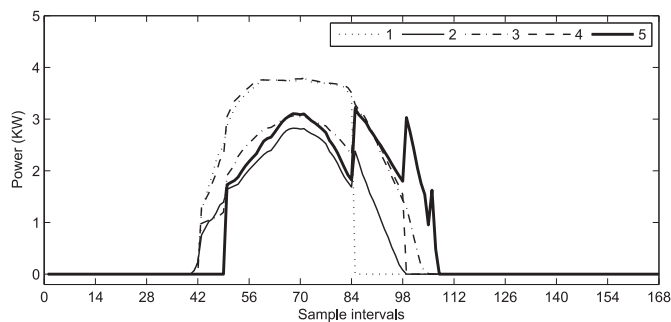


Fig. 9. Power allocation by Algorithm 4.

Fig. 8 demonstrates that Algorithm 4 still optimally flattens the aggregate power curve even though some PHEVs arrive later than others and get an online optimal result. Fig. 9 shows the charging curve of each PHEV, from which we can see the power allocation is also balanced. The three peaks of PHEV 5 after 84 samples are caused by the successive exits of the other four PHEVs because they are charged to their targets ahead of the required times.

C. Simulation Using Realistic Data

The realistic household nonPHEV demand curve has similar pattern to the curve in [6] as described in Fig. 10(a). It is a 24-h data with a sample time of 1 min (i.e., there are 1440 samples for 24 h). Fig. 10(b) is regarded as the predicted household

TABLE III
PARAMETERS OF THE FIVE PHEV MODELS

Model	Battery Size	Energy Need	Max Power
GM-Chevy Volt	16	8	3.84
Nissan-Leaf	24	12	6.6
Tesla-MODEL S	60	30	10
Volvo-C30	24	12	3.52
BMW-Mini E	35	17	11.52

TABLE IV
ENTRY AND EXIT TIMES OF TEN PHEVS

NO.	Model	Entry Time	Exit Time (The next day)
1,6	GM-Chevy Volt	17:00	5:00
2,7	Nissan-Leaf	17:00	7:00
3,8	Tesla-MODEL S	18:00	8:00
4,9	Volvo-C30	23:00	7:00
5,10	BMW-Mini E	24:00	17:00

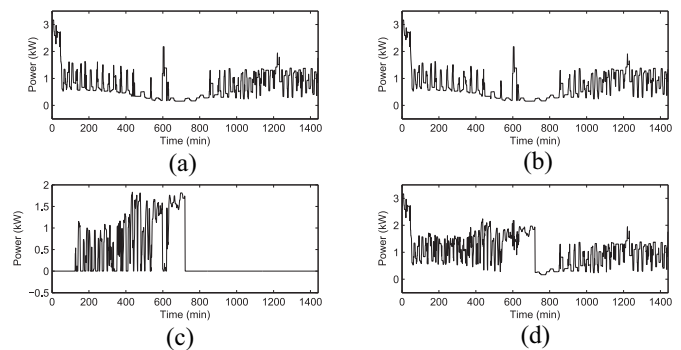


Fig. 10. Power curve of a household. (a) Realistic nonPHEV demand curve of a household. (b) Predicted nonPHEV demand curve of this household. (c) Power allocated to the PHEV of this household. (d) Total power curve of this household.

nonPHEV demand curve and we emulate it by processing the data in Fig. 10(a) with a low-pass filter. Parameters of the five PHEV models are shown in Table III. These data are from [6], [31], and [32]. In the simulation, PHEVs can arrive and leave at different times, as shown in Table IV, and it simulates the interval from 17:00 to 17:00 the next day. The two simulations represent different PHEV penetration levels. The capacity of the transformer is 10 kVA.

1) *Low-Level PHEV Penetration*: In this simulation, we assume there are only five PHEVs, i.e., PHEV 1–5. Fig. 10(c) describes the power allocated to one of the PHEVs using Algorithm 4, and Fig. 10(d) shows the total power curve of this household. It can be seen that no new peak load is created. Fig. 11 shows the total power demand curves with and without DSM. Without DSM, every PHEV starts charging with maximum power as soon as it arrives home. We can see in the figure that not only a new peak load is created (around 500th sample) but also more load is added to a nonPHEV peak load (around 100th sample). Both overload the transformer so much (exceed the 10 kVA capacity) that they can be devastating to the LVT. DSM helps shift the charging timing of PHEVs to when nonPHEV power demand is relatively low.

2) *High-Level PHEV Penetration*: In this simulation, we assume there are ten PHEVs. From Fig. 12, we can see that although the aggregate nonPHEV power demand is below the

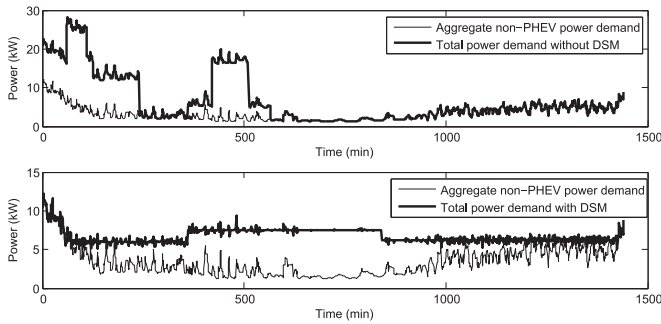


Fig. 11. Power curves of LVT with and without DSM (low-level PHEV penetration).

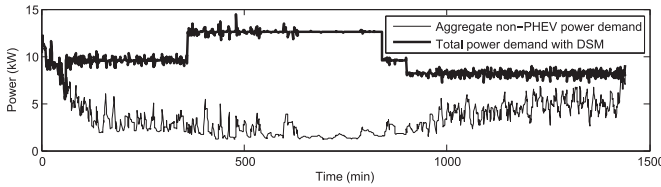


Fig. 12. Power curves of LVT with DSM (high-level PHEV penetration, without the protection mechanism).

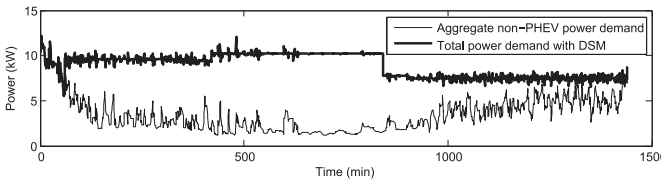


Fig. 13. Power curves of LVT with DSM (high-level PHEV penetration, with the protection mechanism).

capacity of the transformer, the total power demand reach 12 kW and the 20% overloading lasts from around 400th sample to around 800th sample. That is because there is too much PHEV load. To avoid overloading, the protection mechanism in Algorithm 3 kicks in and the energy need of every PHEV is reduced. Fig. 13 shows the effectiveness of the protection mechanism.

V. CONCLUSION

DSM of PHEVs will become necessary to reduce peak loads as the penetration of PHEVs becomes greater. Trying to flatten power-demand curve at transformers will avoid overloading and defer investment. In this paper, we formulate this problem as a convex optimization problem and propose a distributed algorithm, in which the water filling principle plays a pivotal role. Simulation results show that the proposed algorithm can efficiently fulfill the task of flattening the power demand curve and avoid transformer overloading. The water-filling-based algorithm enjoys the following advantages. First, it applies to heterogeneous cases, where PHEVs may have different exit times, energy needs and maximum charging powers. The result is also optimal when PHEVs arrive randomly, so it is of high scalability. Moreover, every PHEV can compute its own power without knowing other PHEVs' information. This algorithm is simple and fast, so it is suitable for engineering practice.

REFERENCES

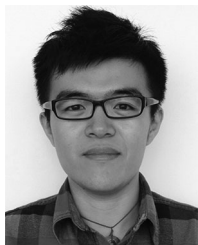
- [1] J. A. P. Lopes, F. J. Soares, and P. M. R. Almeida, "Integration of electric vehicles in the electric power system," *Proc. IEEE*, vol. 99, no. 1, pp. 168–183, Jan. 2011.
- [2] B. Philip *et al.*, "Demand response measurement & verification," White Paper, Association of Edison Illuminating Companies, Mar. 2009.
- [3] C.-T. Li, C. Ahn, H. Peng, and J. S. Sun, "Synergistic control of plug-in vehicle charging and wind power scheduling," *IEEE Trans. Smart Grid*, vol. 28, no. 2, pp. 1113–1121, May 2013.
- [4] Z. Ma, D. S. Callaway, and I. A. Hiskens, "Decentralized charging control of large populations of plug-in electric vehicles," *IEEE Trans. Control Syst. Technol.*, vol. 21, no. 1, pp. 67–78, Jan. 2013.
- [5] L. Gan, U. Topcu, and S. Low, "Optimal decentralized protocol for electric vehicle charging," *IEEE Trans. Power Syst.*, vol. 28, no. 2, pp. 940–951, May 2013.
- [6] S. Shao, M. Pipattanasomporn, and S. Rahman, "Demand response as a load shaping tool in an intelligent grid with electric vehicles," *IEEE Trans. Smart Grid*, vol. 2, no. 4, pp. 624–631, Dec. 2011.
- [7] S. Vandael, N. Boucké, T. Holvoet, and G. Deconinck, "Decentralized demand side management of plug-in hybrid vehicles in a smart grid," in *Proc. 1st Int. Workshop Agent Technol. Energy Syst. (ATES)*, Toronto, ON, Canada, May 2010, pp. 67–74.
- [8] W. Gu, H. Yu, W. Liu, J. Zhu, and X. Xu, "Demand response and economic dispatch of power systems considering large-scale plug-in hybrid electric vehicles/electric vehicles (PHEVs/EVs): A review," *Energies*, vol. 6, no. 9, pp. 4394–4417, Aug. 2013.
- [9] G. C. Goodwin and J. A. De Doná, *Constrained Control and Estimation: An Optimization Approach*. New York, NY, USA: Springer, 2005.
- [10] J. B. Rawlings, "Tutorial overview of model predictive control," *IEEE Control Syst. Mag.*, vol. 20, no. 3, pp. 38–52, Jun. 2000.
- [11] B. De Schutter and R. Scattolini, "Introduction to the special issue on hierarchical and distributed model predictive control," *J. Process Control*, vol. 21, no. 5, pp. 683–684, Jun. 2011.
- [12] R. Martí, D. Sarabia, D. Navia, and C. de Prada, "A method to coordinate decentralized NMPC controllers in oxygen distribution networks," *Comput. Chem. Eng.*, vol. 59, pp. 122–137, Dec. 2013.
- [13] E. Camponogara, D. Jia, B. H. Krogh, and S. Talukdar, "Distributed model predictive control," *IEEE Control Syst. Mag.*, vol. 22, no. 1, pp. 44–52, Feb. 2002.
- [14] M. N. Zeilinger, Y. Pu, S. Rivero, G. Ferrari-Trecate, and C. N. Jones, "Plug and play distributed model predictive control based on distributed invariance and optimization," in *Proc. IEEE 52nd Annu. Conf. Decision Control (CDC)*, Florence, Italy, 2013, pp. 5770–5776.
- [15] W. B. Dunbar and R. M. Murray, "Distributed receding horizon control for multi-vehicle formation stabilization," *Automatica*, vol. 42, no. 4, pp. 549–558, Apr. 2006.
- [16] E. Camponogara and H. F. Scherer, "Distributed optimization for model predictive control of linear dynamic networks with control-input and output constraints," *IEEE Trans. Autom. Sci. Eng.*, vol. 8, no. 1, pp. 233–242, Jan. 2011.
- [17] E. M. Krieger, "Effects of variability and rate on battery charge storage and lifespan," Ph.D. dissertation, Dept. Mech. Aerosp. Eng., Princeton Univ., Princeton, NJ, USA, Apr. 2013.
- [18] Q. Wu *et al.*, "Modeling of electric vehicles (EVs) for EV grid integration study," Paper presented at the 2nd European Conference Smart Grids & E-Mobility, Brussels, Belgium, Oct. 2010.
- [19] E. F. Camacho and C. Bordons, *Model Predictive Control*. New York, NY, USA: Springer, 2013.
- [20] R. Fano, *Transmission of Information*. Cambridge, MA, USA: MIT Press, 1961.
- [21] H. Zhao, A. Yan, C. Zhang, and P. Wang, "An optimizing method based on water-filling for case attribute weight," in *Proc. 24th Chin. Control Decis. Conf.*, Taiyuan, China, 2012, pp. 3455–3458.
- [22] X. S. Zhou, Y. Rui, and T. S. Huang, "Water-filling: A novel way for image structural feature extraction," in *Proc. IEEE Int. Conf. Image Process. (ICIP)*, Kobe, Japan, 1999, pp. 570–574.
- [23] D. Kundur, "Water-filling for watermarking?" in *Proc. IEEE Int. Conf. Multimedia Expo (ICME)*, New York, NY, USA, 2000, pp. 1287–1290.
- [24] J. G. Proakis and M. Salehi, *Digital Communications*, 5th ed. New York, NY, USA: McGraw-Hill, 2008.
- [25] A. Von Meier, *Electric Power Systems: A Conceptual Introduction*. Hoboken, NJ, USA: Wiley, 2006.
- [26] R. R. S. H. Lee Willis, *Aging Power Delivery Infrastructures*, 2nd ed. Boca Raton, FL, USA: CRC Press, 2013.

- [27] E. Sortomme, M. M. Hindi, S. J. MacPherson, and S. Venkata, "Power-factor-corrected single-stage inductive charger for electric vehicle batteries," *IEEE Trans. Ind. Electron.*, vol. 54, no. 2, pp. 1217–1226, Apr. 2007.
- [28] T. Soeiro, T. Friedli, and J. Kolar, "Three-phase high power factor mains interface concepts for electric vehicle battery charging systems," in *Proc. 27th Annu. IEEE Appl. Power Electron. Conf. Expo.*, Orlando, FL, USA, 2012, pp. 2603–2610.
- [29] I. Necoara, V. Nedelcu, and I. Dumitrache, "Parallel and distributed optimization methods for estimation and control in networks," *J. Process Control*, vol. 21, no. 5, pp. 756–766, 2011.
- [30] S. P. Boyd and L. Vandenberghe, *Convex Optimization*. Cambridge, U.K.: Cambridge Univ. Press, 2004.
- [31] Nissan. (2014, Jan.). *Nissan LEAF Electric Car Charging*. [Online]. Available: <http://www.nissanusa.com/electric-cars/leaf/charging-range/charging>
- [32] Tesla. (2014, Jan.). *Features and Specs*. [Online]. Available: <http://www.teslamotors.com/models/features#/battery>



Yuting Mou received the Bachelor's degree in electrical engineering from Jilin University, Changchun, China, in 2012. He is currently pursuing the master's degree from the Department of Control Science and Engineering, Zhejiang University, Hangzhou, China.

His current research interests include smart grid and distributed optimization.



Hao Xing (S'14) received the Bachelor's degree in electrical engineering from Zhejiang University, Hangzhou, China, in 2012, where he is currently pursuing the Ph.D. degree from the Department of Control Science and Engineering.

His current research interests include distributed control and optimization in smart grid.



Zhiyun Lin (SM'10) received the Bachelor's and Master's degrees in electrical engineering from Yanshan University, Qinhuangdao, China, and Zhejiang University, Hangzhou, China, in 1998 and 2001, respectively, and the Ph.D. degree in electrical and computer engineering from the University of Toronto, ON, Canada, in 2005.

From 2005 to 2007, he was at the Department of Electrical and Computer Engineering, University of Toronto, as a Post-Doctoral Research Associate. He joined the College of Electrical Engineering, Zhejiang University, in 2007, where he is currently a Professor of Systems Control. He is also with the State Key Laboratory of Industrial Control Technology, Zhejiang University, and was also a Visiting Professor at several universities, including the Australian National University, Canberra, ACT, Australia; the University of Cagliari, Cagliari, Italy; the University of Newcastle, Callaghan, NSW, Australia; and the University of Technology Sydney, Ultimo, NSW. His current research interests include distributed control, estimation and optimization, coordinated and cooperative control of multiagent systems, hybrid and switched system theory, and locomotion control of biped robots.

Prof. Lin is currently an Associate Editor of the *Hybrid Systems: Nonlinear Analysis and International Journal of Wireless and Mobile Networking*.



Minyue Fu (F'03) received the Bachelor's degree in electrical engineering from the University of Science and Technology of China, Hefei, China, in 1982, and the M.S. and Ph.D. degrees from the University of Wisconsin–Madison, Madison, WI, USA, in 1983 and 1987, respectively.

From 1987 to 1989, he was an Assistant Professor at Wayne State University, Detroit, MI, USA. He joined the University of Newcastle, Callaghan, NSW, Australia, in 1989, and was promoted to Chair Professor in 2002. He has served as the Head of Department for Electrical and Computer Engineering and the Head of the School of Electrical Engineering and Computer Science over seven years. He has been a Visiting Professor at the University of Iowa, Iowa City, IA, USA; Nanyang Technological University, Singapore; and Tokyo University, Bunkyo, Tokyo. He has held a Changjiang Visiting Professorship at Shandong University, Jinan, China, and a Qian-Ren Professorship at Zhejiang University, Hangzhou, China. His current research interests include control systems, signal processing, communications, networked control systems, and smart electricity networks. He has published nearly 350 papers, including over 120 journal papers.

Prof. Fu has been an Associate Editor of the *IEEE TRANSACTIONS ON AUTOMATIC CONTROL*, the *IEEE TRANSACTIONS ON SIGNAL PROCESSING*, *Automatica*, and the *Journal of Optimization and Engineering*.